A Gene Controlling Variation in Arabidopsis Glucosinolate Composition Is Part of the Methionine Chain Elongation Pathway[1]

Juergen Kroymann, Susanne Textor, Jim G. Tokuhisa, Kimberly L. Falk, Stefan Bartram, Jonathan Gershenzon*, and Thomas Mitchell-Olds

Departments of Genetics and Evolution (J.K., T.M.-O.), Plant Biochemistry (S.T., J.G.T., K.L.F., J.G.), and Bioorganic Chemistry (S.B.), Max Planck Institute for Chemical Ecology, Carl-Zeiss-Promenade 10, 07745 Jena, Germany

Arabidopsis and other Brassicaceae produce an enormous diversity of aliphatic glucosinolates, a group of methionine (Met)-derived plant secondary compounds containing a β-thio-glucose moiety, a sulfonated oxime, and a variable side chain. We fine-scale mapped *GSL-ELONG*, a locus controlling variation in the side-chain length of aliphatic glucosinolates. Within this locus, a polymorphic gene was identified that determines whether Met is extended predominantly by either one or by two methylene groups to produce aliphatic glucosinolates with either three- or four-carbon side chains. Two allelic mutants deficient in four-carbon side-chain glucosinolates were shown to contain independent missense mutations within this gene. In cell-free enzyme assays, a heterologously expressed cDNA from this locus was capable of condensing 2-oxo-4-methylthiobutanoic acid with acetyl-coenzyme A, the initial reaction in Met chain elongation. The gene *methylthioalkylmalate synthase1* (*MAM1*) is a member of a gene family sharing approximately 60% amino acid sequence similarity with 2-isopropylmalate synthase, an enzyme of leucine biosynthesis that condenses 2-oxo-3-methylbutanoate with acetyl-coenzyme A.

Glucosinolates are a prominent and diverse class of plant secondary metabolites in Arabidopsis and other genera of the Brassicaceae (Halkier, 1999; Rask et al., 2000). Their general structure has two common domains, a β-thio-Glc moiety and a sulfonated oxime, plus a variable side chain derived from one of several amino acids. When plant tissue is damaged, glucosinolates come into contact with endogenous β-thioglucosidases, known as myrosinases. The resulting aglycones are unstable and rearrange to form isothiocyanates, nitriles, thiocyanates, epithionitriles, and other substances (Bones and Rossiter, 1996).

In Arabidopsis, most glucosinolates contain a variable side chain derived from chain-elongated derivatives of Met containing one to six additional methylene groups (Hogge et al., 1988). Although these additional methylene groups appear to arise from acetyl-coenzyme A (CoA), the side chain is not formed by direct fusion of C_2 acetate units as in fatty acid biosynthesis but by an acetyl-CoA condensation/decarboxylation cycle that results in the net addition of one methylene group for each turn of the cycle (Graser et al., 2000). Based largely on in vivo studies with isotopically labeled tracers (Chisholm and Wetter, 1964; Matsuo and Yamazaki, 1964; Chapple et al., 1988; Haughn et al., 1991; Graser et al., 2000), the Met chain elongation pathway is thought to be initiated by the transamination of Met to form the corresponding 2-oxo acid (Chapple et al., 1990). This is followed by a three-step chain elongation cycle consisting of condensation of the 2-oxo acid with acetyl-CoA, isomerization, and oxidative decarboxylation (Fig. 1). The net result is a 2-oxo acid extended by one methylene group. The newly formed 2-oxo acid can be transaminated to form homo-Met or undergo additional cycles of chain elongation (Fig. 1). After elongation, the extended Met homologs enter the reaction sequence that creates the core structure of glucosinolates, i.e. conversion of the amino acid to an oxime, addition of a thiol moiety, formation of a β-thioester bond with Glc, and sulfonation of the oxime group (Halkier and Du, 1997). Finally, further side-chain modifications can occur.

Several Met-derived glucosinolates have significance in human health and agriculture. For instance, 4-methylsulfinylbutyl glucosinolate is hydrolyzed by myrosinase action to the isothiocyanate sulforaphane [1-isothiocyanato-4-(methylsulfinyl)butane], which is a strong inducer of phase II detoxification enzymes known to be of major importance in cancer protection (Zhang et al., 1992; Nastruzzi et al., 1996; Fahey et al., 1997). 2-Hydroxybut-3-enylglucosinolate, whose
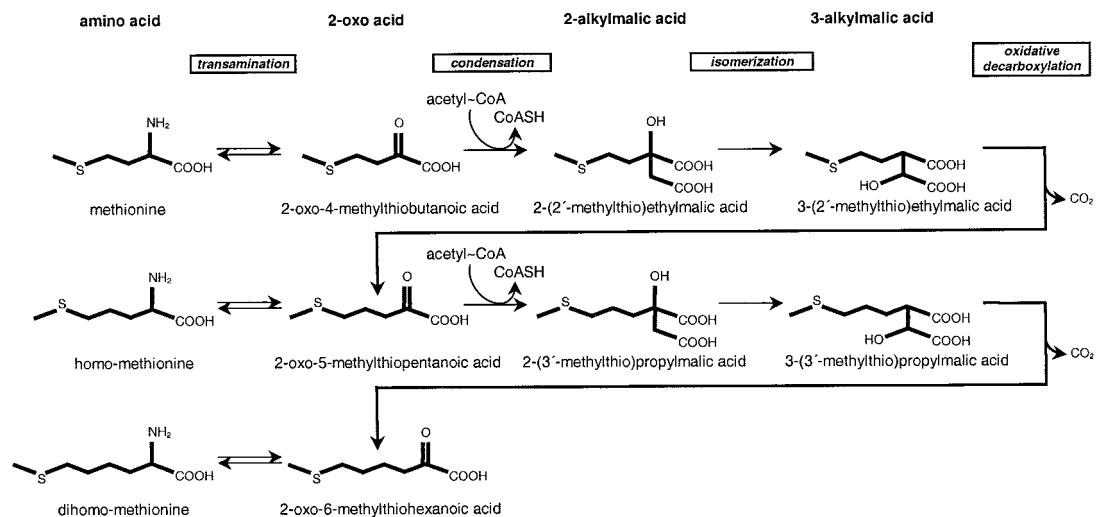

Figure 1. Postulated Met chain elongation pathway in glucosinolate biosynthesis. Shown are reaction steps and chemical structures for the first two rounds of chain elongation. The 2-oxo acid products are substrates for either transamination or subsequent condensation reactions.

main hydrolysis product is 5-vinyloxazolidine-2-thione, has been identified as the goitrogenic component of rapeseed meal (Bradshaw et al., 1984). Glucosinolates and their breakdown products also may protect plants against pathogens (Doughty et al., 1991), regulate the feeding behavior of herbivores (Blau et al., 1978; Bodnaryk, 1991; Brown and Morra, 1995; Donkin et al., 1995; Giamoustaris and Mithen, 1995), and influence the oviposition preferences of insects (Reed et al., 1989; Du et al., 1995; Städler et al., 1995; Justus and Mitchell, 1996).

Arabidopsis ecotypes vary remarkably in their composition of Met-derived glucosinolates (Magrath et al., 1994; Kliebenstein et al., 2001) One major locus responsible for this variation was termed *GSL-ELONG* due to its ability to determine the degree of elongation of the side chain of Met-derived glucosinolates (Magrath et al., 1994). The predominant aliphatic glucosinolate in leaves of Landsberg *erecta* (L*er*) is 3-hydroxypropyl glucosinolate, whereas in Columbia (Col-0) the leaves accumulate primarily 4-methylsulfinylbutyl glucosinolate. Thus, most aliphatic leaf glucosinolates in L*er* have a basic side chain with three methylene groups (derived from homo-Met) and are termed "C_3" glucosinolates, whereas those in Col-0 have a basic side chain with four methylene groups (derived from dihomo-Met) and are termed "C_4" glucosinolates. This represents one and two cycles of chain elongation, respectively. In addition, lesser amounts of longer chain aliphatic glucosinolates are detectable in the leaves of both of these ecotypes. Six Col-0 mutants have been isolated that are altered in glucosinolate accumulation and two of these mutant lines, TU1 and TU5, were deficient in C_4 glucosinolates (Haughn et al., 1991).

GSL-ELONG recently was mapped to a region of approximately 140 kb near the top of chromosome V (Campos et al., 2000). This region has two candidate genes with similarity to genes encoding 2-isopropylmalate synthase (IPMS), an enzyme that catalyzes a condensation reaction in Leu biosynthesis analogous to the condensation reactions between 2-oxo acids and acetyl-CoA occurring in Met chain elongation. Here, we use fine-scale mapping to identify which member of this gene family is responsible for the C_3/C_4 chain length variation of Met-derived glucosinolates. We also demonstrate that the Col-0 allele of this gene, named *MAM1*, codes for a methylthioalkylmalate synthase capable of condensing 2-oxo-4-methylthiobutanoic acid (OMTB) with acetyl-CoA to form 2-(2'-methylthio)ethylmalic acid (MTEM), the initial reaction in Met chain elongation. Moreover, we show that the mutant lines TU1 and TU5 harbor missense mutations in *MAM1*, reinforcing the conclusion that MAM1 plays a vital role in Met chain elongation in Arabidopsis.

RESULTS

IPMS-Like Genes in Arabidopsis

To aid in cloning the gene for the initial condensation step in the chain elongation of Met-derived glucosinolates (Fig. 1), the Arabidopsis genome was searched for genes with similarity to those encoding IPMS, which catalyzes a very similar condensation reaction in Leu biosynthesis. Four candidate genes were found, two of which are at the *GSL-ELONG* locus, a locus controlling glucosinolate side-chain length that maps near the top of chromosome V (Magrath et al., 1994; Campos et al., 2000). Based on the results described below, we have named these two genes *MAM1* (encoding a methylthioalkylmalate synthase, see below) and *MAM-L* (MAM synthase-
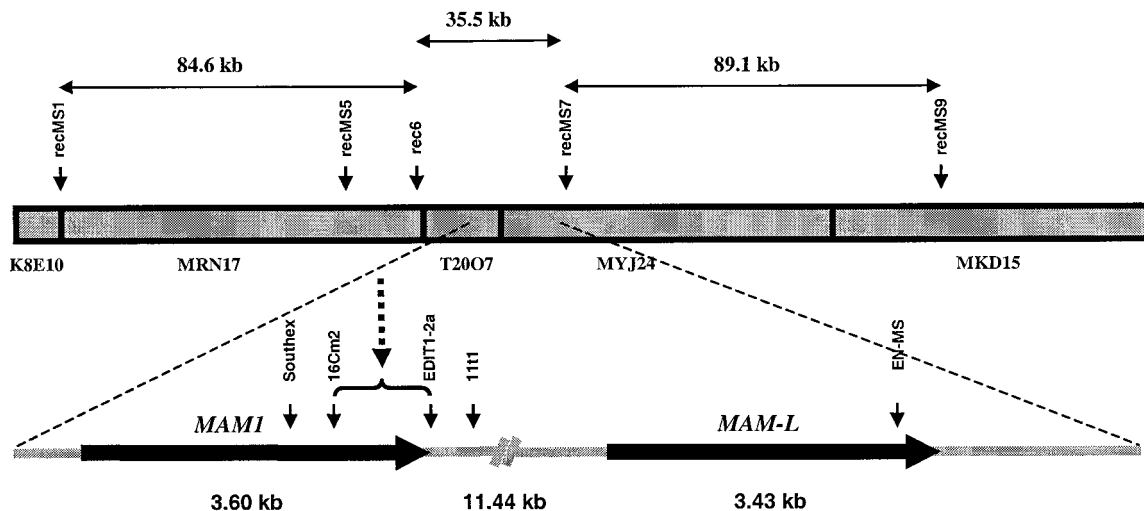
Figure 2. Fine-scale mapping of *GSL-ELONG*. The DNA sequence of the *GSL-ELONG* region of chromosome V (outlined bar) was derived from the nonoverlapping sequences of K8E10, MRN17, T2O7, MYJ24, and MKD15 (GenBank accession nos. AB025618, AB005243, AB026660, AB006708, and AB007648). Vertical solid arrows labeled recMS1, rec6, recMS7, and recMS9 indicate the primer pair markers used for mapping the *GSL-ELONG* phenotype. The approximate sizes of intervals between these markers (horizontal arrows) are based on the Col-0 ecotype. Below, the region encompassing the *MAM1* and *MAM-L* genes (thick horizontal arrows) is enlarged. Their approximate sizes and the size of the interval separating them are shown underneath. Additional primers and markers used to identify recombination points are indicated by vertical black arrows labeled Southex, 16Cm2, EDIT1-2a, 11t1, and EN-MS. The dashed vertical arrow indicates the recombination point which distinguishes functional effects of the *MAM1* and *MAM-L* genes in family 5 (Table II).

like). *MAM1* and *MAM-L* are arranged head to tail on bacterial P1 clones of genomic Arabidopsis DNA T2O7 and MYJ24, respectively, and are separated by 11.5 kb of intervening sequence, as shown in Figure 2.

The other two sequences with high similarity to those encoding IPMS are on chromosome I. The first, designated *F15H18.3* (accession no. AC013354.6), is located on top of chromosome I near the marker g15785. The second, *F2P9.9* (accession no. AC016662.5), maps at the bottom of chromosome I close to the marker PAB5. The annotated exon-intron structure of these sequences was confirmed by sequence analysis of the respective cDNAs. Although the gene structure predicted by *F2P9.9* was confirmed, two short insertions of 29 and 15 amino acids in the open reading frame (ORF) defined by *F15H18*.3 were shown to be artifacts of the gene prediction program. Thus, both the corrected *F15H18.3* and *F2P9.9* comprise 12 exons, whereas *MAM1* and *MAM-L* consist of 10 exons as confirmed by sequencing of the corresponding cDNAs (Fig. 3). The *MAM1* and *MAM-L* genes lack exons 10, 11, and part of 12 from *F15H18.3* or *F2P9.9*. In addition, the first exon of the *IPMS*-like genes on chromosome I is homologous to both exons 1 and 2 of *MAM1* and *MAM-L* on chromosome V (Fig. 3).

The derived protein sequences from all four Arabidopsis IPMS-like genes contain an N-terminal extension of approximately 80 amino acids not present in bacterial IPMS sequences. The first 50 to 60 amino acids of this extension show the typical features of organellar targeting sequences, i.e. a high proportion

of Ser and Thr residues and a low proportion of acidic residues (von Heijne et al., 1989; Emanuelsson et al., 1999). To better understand the evolutionary relationship of these genes, we performed a cluster analysis of the deduced amino acid sequences of *IPMS* and *IPMS*-like genes from Arabidopsis (four), tomato (*Lycopersicon pennellii*; two), and *Synechocystis* sp. PCC 6803 (one). The archaebacterial *Methanococcus jannaschii* sequence was used as an out-group. The analysis reveals that the Arabidopsis F15H18.3 and F2P9.9 are more closely related to one another and to the IPMSs from tomato than to either MAM1 or MAM-L. Because all plant species presumably possess at least one *IPMS* gene that encodes the
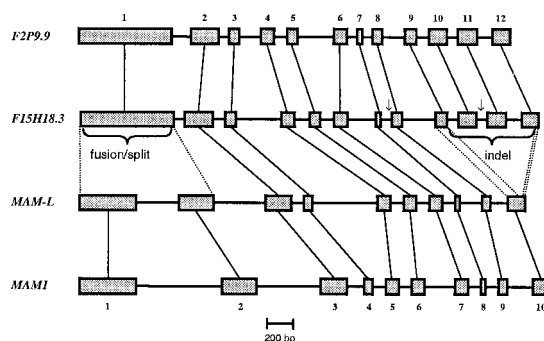

Figure 3. Exon-intron structure of *IPMS*-like genes in Arabidopsis. Shown are exons (thick bars) and introns (thin bars) from start to stop of the ORF. Vertical thin lines connect homologous exons. Arrows indicate deviations from the predicted exon-intron structure of *F15H18.3*, as detected in the respective cDNAs.

enzyme functioning in Leu biosynthesis, *F15H18.3* and/or *F2P9.9* would appear to encode IPMS. Thus, *MAM1* or *MAM-L* are the most likely candidates to be involved in glucosinolate chain elongation.

MAM1 Is Responsible for the C_3/C_4 Chain Length Variation of Met-Derived Glucosinolates

To determine which of the candidate sequences, *MAM1* or *MAM-L*, controls C_3/C_4 chain length variation in the biosynthesis of Met-derived glucosinolates, a set of approximately 5,000 F_2 progeny from a cross between the Col-0 wild type and the recombinant inbred line CL5 (Lister and Dean, 1993) was analyzed for recombination in the *GSL-ELONG* region. The CL5 line carries the L*er* allele at *GSL-ELONG* (Mithen et al., 1995). Of approximately 4,600 plants (equal to 9,200 independent gametes) that were scorable, a total of 95 plants were recombinant between markers recMS1 and recMS9 (Fig. 2). These were further genotyped at markers rec6 and recMS7, which flank *MAM1* and *MAM-L*. For 93 plants, the recombination point could be placed in intervals between recMS1 and rec6, rec6 and recMS7, or recMS7 and recMS9, as shown in Table I. On average, a recombination occurred every 2.2 kb. However, only two plants were recombinant in the 35.5-kb interval between markers rec6 and recMS7, indicating that recombination is suppressed around this region in Col-0 $\times$ CL5 ($\chi^2 = 18.6851$, degrees of freedom = 2, and $P < 0.0001$).

Leaf glucosinolates were analyzed in a subset of recombinant F_3 plants confirmed homozygous in the *GSL-ELONG* region. Plants carrying the Col-0 alleles at *MAM1* and *MAM-L* accumulated C_4 glucosinolates, whereas plants carrying the L*er* alleles at these genes formed predominantly C_3 glucosinolates (Table II, Fig. 4). Glucosinolate profiles were unaffected by recombinations in either the region 5' of *MAM1* between markers recMS1 and rec6 (Table II, Families 6, 7 and 8) or the region 3' of *MAM-L* between recMS7 and recMS9 (Table II, Families 1–4 and 9–14).

Table I. *Fine-scale mapping of the GSL-ELONG region*

Approximately 4,600 F_2 plants (equal to 9,200 independent gametes) were scored. The observed recombination frequency is 1%. Thus, the investigated interval equals 1 cM. Note that recombination in the interval comprising the *GSL-ELONG* locus (between markers rec6 and recMS7) is suppressed.

Interval	Size	No. of Recombinants	Recombinants
	kb		*kb*
recMS1–rec6	84.6	36	0.43
rec6–recMS7	35.5	2	0.06
recMS7–recMS9	89.1	55	0.62
Undetermined	–	2	–
Total	209.2	95	0.45

The two F_2 plants with recombinations in the interval flanked by the markers rec6 and recMS7 were subjected to further analysis. One of these plants was recombinant between markers EN-MSrev and recMS7 (Fig. 2), and the other had recombined between markers 16Cm2 and EDIT1-2a (Fig. 2). Only the latter plant harbors a recombination point separating the *MAM1* and *MAM-L* candidate genes. This genotype is homozygous Col-0 at recMS1, rec6 ,and for at least 73% of the *MAM1* gene (Fig. 2), but heterozygous at *MAM-L*, recMS7, and recMS9. Leaves of this plant form predominantly C_4 glucosinolates. Also, its F_3 progeny, verified to be homozygous for this recombination (i.e. homozygous L*er* at *MAM-L*, recMS7, and recMS9), accumulate C_4 glucosinolates (Fig. 4, Table II, Family 5). Thus, the allelic state of *MAM1* is responsible for the C_3/C_4 chain length variation of Met-derived glucosinolates.

The Phenotypes of TU1 and TU5 Are Associated with Mutations in *MAM1*

The mutant lines TU1 and TU5, derived from the Col-0 ecotype, carry allelic *gsm1* mutations (Haughn et al., 1991). To confirm their phenotype, leaf glucosinolate content was analyzed and compared with Col-0 wild type. The HPLC chromatogram of the TU1 line showed greatly reduced levels of 4-methylsulfinylbutyl glucosinolate (Table III), and an absence of 4-methylthiobutyl, 5-methylsulfinylpentyl, and 6-methylsulfinyl glucosinolates (Table III), consistent with the original description. Coincident with these losses was an increase in the C_3 glucosinolates, 3-methylsulfinylpropyl and 3-methylthiopropyl (Table III). A qualitatively similar glucosinolate profile was obtained from TU5 (Table III). This pattern of changes in glucosinolate chain length would be expected from a defect in the conversion of a C_3 to a C_4 glucosinolate precursor. To establish whether the *gsm1* mutants and the L*er* *MAM1* locus were allelic, the leaf glucosinolate profiles were determined in the F_1 generation of crosses between L*er* and either TU1 or TU5. The absence of C_4 glucosinolates in F_1 progeny indicated a lack of complementation. Thus, the biosynthetic lesions in the conversion of C_3 to C_4 glucosinolate precursors in the mutants are the same as in the L*er* ecotype, indicating that *gsm1* is probably allelic with *MAM1*.

To confirm the allelism, cDNAs corresponding to the *MAM1* and *MAM-L* ORFs of Col-0, TU1, and TU5 were sequenced. Although no differences were detected in the *MAM-L* gene, both of the mutant lines exhibited a single transition mutation in *MAM1* (Fig. 5). The TU1 line had a base substitution of adenine for the wild-type guanine at position 868 relative to the start of the ORF (G868A). The TU5 line had a transition from cytosine to thymine at position 305 relative to the start (C305T). These base substitutions are consistent with the mutagenic properties of the

Table II. *Col-0 (C) and Ler (L) allelic state and side-chain length of the predominant glucosinolates in recombinant F₃ families*

F₃ plants derived from Col-0 × CL5 F₂ plants with recombination events between recMS1 and recMS9 were confirmed for homozygosity, and glucosinolates were analyzed. In general, several plants were analyzed per family. L, Plants carried the Ler-0 allele at the respective locus; C, plants harbored the Col-0 allele. C_3, Predominant glucosinolates are derived from homo-Met; C_4, plants accumulate glucosinolates derived from dihomo-Met. Note that plants from family 5 harbor a recombination between *MAM-1* and *MAM-L*.

F₃ Family No.	Allelic State 5' of *GSL-ELONG*	Allelic State at *MAM1*	Allelic State at *MAM-L*	Allelic State 3' of *GSL-ELONG*	Predominant Glucosinolate Type
1	C	C	C	L	C_4
2	C	C	C	L	C_4
3	C	C	C	L	C_4
4	C	C	C	L	C_4
5	C	C	L	L	C_4
6	L	C	C	C	C_4
7	C	L	L	L	C_3
8	C	L	L	L	C_3
9	L	L	L	C	C_3
10	L	L	L	C	C_3
11	L	L	L	C	C_3
12	L	L	L	C	C_3
13	L	L	L	C	C_3
14	L	L	L	C	C_3

alkylating reagent ethylmethane sulfonate used to generate the mutants.

Both base changes are predicted to cause missense mutations. In the *gsm1-1* allele from TU1, the nucleotide change G868A would convert an Ala codon to a Thr (A290T) and introduce a polar residue within a stretch of hydrophobic amino acids. The *gsm1-2* allele from TU5 is predicted to cause a change from a wild-type Ser to a Phe at position 102 (S102F). The fact that the *gsm1* mutants with altered levels of C_3/C_4 glucosinolates both possess a nonconservative amino acid substitution in MAM1 supports the hypothesis that this gene controls the variation between C_3 and C_4 glucosinolates.

The Col-0 MAM1 Polypeptide Is Capable of Condensing a 2-Oxo Acid with Acetyl-CoA to Form a 2-Alkylmalate Derivative

The initial reaction of the Met chain elongation pathway involves the condensation of a 2-oxo-acid derived from Met with acetyl-CoA to form a 2-methylthioalkylmalate derivative (Fig. 1). To demonstrate directly that the *MAM1* gene encoded an enzyme capable of catalyzing such a reaction, the Col-0 allele was expressed in *Escherichia coli*. Bacterial cells containing an overexpression construct were disrupted by sonication and the resulting supernatant was assayed with [1-^{14}C]acetyl-CoA and OMTB, the oxo-acid derived from the deamination of Met (Fig. 6). A novel peak was detected that was coincident with the retention time of an authentic standard of MTEM, the expected product of the condensation reaction (Fig. 1). This novel peak was absent in assays with heat-denatured enzyme or without the 2-oxo acid cosubstrate, and was also not detected in extracts from *E. coli* lacking the expression construct. Activity was maximal at pH 8.5 and required a divalent metal ion, such as Mn^{2+}. The identity of the biosynthetic product was confirmed by liquid chromatography-mass spectrometry (LC-MS) analyses that gave a mass spectrum identical to that of the authentic standard. Assays of the MAM1 protein expressed from both Ler and the mutant line TU1, performed under identical conditions as assays for Col-0 MAM1, did not show this condensation activity. Thus, bacterial expression of *MAM1* cDNAs showed that expression constructs with the sequence from Col-0, but not from Ler or TU1, encoded a protein capable of using acetyl-CoA and the 2-oxo-derivative of Met to catalyze the initial condensation reaction in the chain elongation of glucosinolates. This activity was also absent when *MAM-L* from Ler was expressed and assayed under the same conditions.

DISCUSSION

The Role of *MAM1* in Met Chain Elongation

In recent years, an effort to map genes controlling glucosinolate variation in Arabidopsis has identified a locus on the upper arm of chromosome V that regulates the side chain length of Met-derived glucosinolates (Magrath et al., 1994). This locus, *GSL-ELONG*, controls the accumulation of glucosinolates with C_3 versus C_4 side chains. It was mapped to a 140-kb region encompassing two genes that had approximately 60% identity at the amino acid level with enzymes, such as isopropylmalate synthase and homocitrate synthase, that condense acetyl-CoA with 2-oxo acids (Campos et al., 2000). These two genes in the *GSL-ELONG* region (*MAM1* and *MAM-L*) were found to be highly homologous and within 11.5 kb of each other. In this report, we have determined that one of these genes (*MAM1*) controls side-chain length
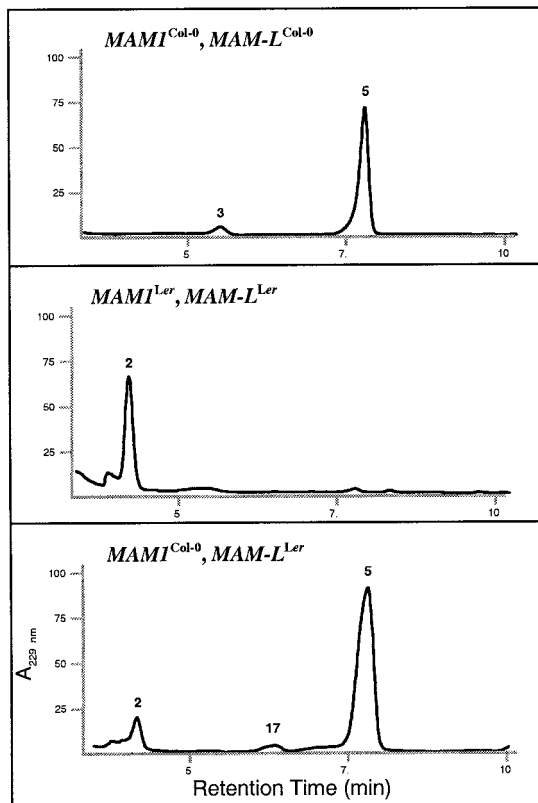
Figure 4. HPLC chromatograms of glucosinolate profiles from Col-0 × CL5 F$_3$ recombinant plants. Glucosinolates were extracted and separated as described in "Materials and Methods," and identified by their retention times and UV spectra. Shown are signals from 3.5- to 10-min retention time during which time all of the glucosinolates eluted that varied in these crosses. Amounts are given in relative absorption units. The allelic state at *MAM1* and *MAM-L* is indicated in the upper left corners. Specific glucosinolates are identified by numbers that correspond to Table III.

variation in glucosinolate biosynthesis and encodes a condensing activity using acetyl-CoA and the 2-oxo derivative of Met as substrates. This is the first reaction of the Met chain elongation cycle and is closely analogous to the condensation of acetyl-CoA and 2-oxo-3-methylbutanoate in Leu biosynthesis.

Evidence for the role of *MAM1* in Met chain elongation is based on mapping experiments in which an individual genotype was identified that had a recombination between the two *IPMS*-like genes in the *GSL-ELONG* region. Glucosinolate profile was controlled by the *MAM1* locus rather than *MAM-L*. This finding was confirmed by the presence of independent missense mutations at the *MAM1* locus of the two allelic mutant lines, TU1 and TU5, which also possessed altered glucosinolate chain length profiles. In both of these mutants, the *MAM-L* locus had a wild-type sequence. In addition, the mutant lines were unable to complement the naturally occurring lack of C$_4$ glucosinolates in crosses with the L*er* ecotype, suggesting that chain length control in both

L*er* and these mutants is mediated by a common locus.

Heterologous expression of the Col-0 *MAM1* allele in *E. coli* revealed that this gene encoded an enzyme capable of condensing acetyl-CoA with the Met derivative, OMTB, to produce MTEM, the first step in the C$_2$ to C$_3$ elongation cycle of Met chain elongation. Although we surmise that the *MAM1* enzyme can also catalyze the condensation step in the C$_3$ to C$_4$ extension cycle, the lack of commercial availability of the requisite substrate, 2-oxo-5-methylthiopentanoic acid, has so far precluded its direct demonstration. Nevertheless, the molecular and genetic evidence for the role of the Col-0 *MAM1* allele in regulating the abundance of both C$_3$ and C$_4$ glucosinolates is compelling.

To date, our results do not yet suggest a candidate gene for the condensation step in the C$_2$ to C$_3$ elongation cycle in L*er* and the TU1 and TU5 mutants, both of which accumulate C$_3$ glucosinolates and so must perform this reaction. Heterologously expressed MAM1 from L*er*, TU1 and TU5, along with *MAM-L* from L*er* were not capable of catalyzing this activity when tested with the same substrates and under identical conditions to those that promoted the condensation reaction of MAM1 from Col-0. The other two *IPMS*-like genes in Arabidopsis have high similarity to *IPMS*-like genes from non-glucosinolate-forming species and are expected to be involved in Leu formation. However, these may also encode proteins capable of performing the initial condensation step in the C$_2$ to C$_3$ elongation cycle of glucosinolate biosynthesis, a possibility presently under investigation.

The accumulation of Met-derived C$_4$ glucosinolates in Col-0 versus the accumulation of C$_3$ glucosinolates in L*er* is a result of a polymorphism in a gene encoding the condensation step of Met chain elongation. In principle, such a metabolic difference could also result from differences in other aspects of the biosynthetic pathway, such as the substrate specificity of the aminotransferase responsible for converting chain-extended 2-oxo acids to their corresponding amino acids after elongation, or the transport of intermediates (Haughn et al., 1991). However, the three independent experimental approaches taken here (mapping, mutant analysis, and heterologous expression) all indicate that the *GSL-ELONG* polymorphism in Arabidopsis is due solely to the presence or absence of the Col-0 *MAM1* allele.

It has been assumed that a single series of chain extensions generates all of the chain-elongated variants of Met (Haughn et al., 1991). However, despite the dramatic change in C$_3$, C$_4$, C$_5$, and C$_6$ glucosinolates in the TU1 and TU5 mutant lines, the levels of C$_7$ and C$_8$ glucosinolates in these plants are largely unaffected. Thus, C$_7$ and C$_8$ Met-derived glucosinolates are likely to be formed by a pathway that is at least partially independent from that forming shorter

Table III. *Glucosinolate content (micromole per gram dry wt) in mutant and wild-type Arabidopsis*

SEs are given in parentheses. Expanding leaves were harvested just prior to bolting and extracted as described in "Materials and Methods." Each analysis consisted of leaves from five pooled plants. All lines were analyzed three to four times, except for TU5 and Ler × TU1, which were analyzed only once.

No.	Glucosinolate[a]	Col-0	TU1 (gsm1-1)	TU5 (gsm1-2)	Ler	Ler × TU1
1	2-MSO-ethyl	0.0	0.8(0.1)	0.1	0.0	0.0
2	3-OH-propyl	0.0	0.0	0.0	63.3(3.3)	14.5
3	3-MSO-propyl	3.8(0.2)	16.1(0.8)	25.5(1.8)	1.7(0.3)	0.0
4	3-MT-propyl	0.0	0.2(0.0)	0.3(0.1)	0.1(0.0)	0.0
5	4-MSO-butyl	22.6(1.6)	0.4(0.0)	2.7(0.1)	0.4(0.0)	0.0
6	4-MT-butyl	2.8(0.2)	0.0	0.4(0.2)	0.0	0.0
7	5-MSO-pentyl	0.6(0.0)	0.0	0.0	0.0	0.0
8	6-MSO-hexyl	0.2(0.0)	0.0	0.0	0.0	0.0
9	7-MSO-heptyl	0.7(0.1)	0.5(0.1)	0.3(0.0)	0.4(0.0)	0.1
10	7-MT-heptyl	0.2(0.0)	0.1(0.0)	0.0	0.2(0.0)	0.0
11	8-MSO-octyl	4.1(0.2)	5.9(0.3)	4.6(0.4)	7.8(0.6)	1.9
12	8-MT-octyl	0.4(0.2)	1.1(0.1)	0.3(0.1)	1.3(0.1)	0.1
13	4-OH-indol-3-ylmethyl	0.3(0.1)	0.3(0.0)	0.0	0.1(0.0)	0.0
14	Indol-3-ylmethyl	6.8(0.9)	11.0(0.7)	4.4	5.9(0.7)	1.5
15	4-MO-indol-3-ylmethyl	0.5(0.0)	0.6(0.0)	0.9	0.5(0.0)	0.3
16	1-MO-indol-3-ylmethyl	3.7(1.2)	3.1(1.0)	0.1	1.6(0.3)	0.1
17	4-OH-butyl	0.0	0.0	0.0	0.0	0.0

[a] MSO, Methylsulfinyl; OH, hydroxy; MT, methylthio; MO, methoxy.

chain glucosinolates. *MAM-L* and/or other, undescribed loci may encode the condensing activities involved in the formation of the longer chain glucosinolates.

Side-Chain Elongation and Glucosinolate Diversity

Met-derived glucosinolates in Arabidopsis can undergo one to six cycles of chain elongation resulting in the formation of C_3 through C_8 glucosinolates. Chain elongation greatly increases the range and chemical properties of possible glucosinolate structures and their hydrolytic derivatives. For example, upon myrosinase action longer chain glucosinolates might be expected to produce hydrolysis products that are much less polar and less volatile than those from shorter chain glucosinolates. Later side-chain modifications, including thiol oxidation, desulfation, hydroxylation, and esterification further increase the chemical diversity of glucosinolates produced from Met. Diversity might play a role in reducing the impact of herbivores that have evolved tolerance to a particular glucosinolate profile. Thus, the *MAM1* locus and other genes that function in chain elongation may have evolutionary and ecological significance.

Recruitment of Glucosinolate Biosynthetic Genes from Primary Metabolism

Cluster analysis of IPMS-like sequences reveals that *MAM1* and *MAM-L* are probably derived from ancestral *IPMS* genes. Therefore, following an initial gene duplication of *IPMS*, one of the resulting copies may have acquired a new capacity in secondary metabolism, whereas the other locus retained its function in Leu biosynthesis. Subsequent gene duplications gave rise to *F15H18.3* and *F2P9.9*, on one hand, and *MAM1* and *MAM-L*, on the other.

After IPMS, three additional enzymes are involved in the later steps of Leu biosynthesis: 2-isopropylmalate isomerase (dehydratase), 3-isopropylmalate dehydrogenase, and Leu aminotransferase. These catalyze reactions analogous to the remaining steps in Met chain elongation: isomerization, oxidative decarboxylation, and transamination (Fig. 1). It is tempting to speculate that duplication of the remaining Leu biosynthetic genes gave rise to copies that acquired an analogous function in Met chain elongation. Leu biosynthesis in higher plants takes place in the chloroplast, and IPMS is situated in the thylakoids (Hagelstein and Schultz, 1993; Hagelstein et al., 1997). Because all of the IPMS-like sequences, F15H18.3, F2P9.9, MAM1, and *MAM-L*, have putative chloroplast targeting sequences and, furthermore, because biochemical studies have demonstrated that methylthioalkylmalate synthase activity is localized in the chloroplast (K. Falk and J. Gershenzon, unpublished data), it is likely that Met chain elongation also occurs at this subcellular site.

Fine-Scale Mapping as a Means to Dissect Function within Gene Clusters

When gene families are arranged in tightly linked clusters, identifying the function of individual genes is a major challenge. Members of gene families often share sufficient sequence similarity to prevent antisense or overexpression studies from successfully distinguishing between them. Although T-DNA or transposon-tagged mutants can provide ready access
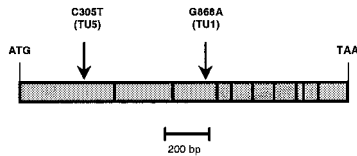
Figure 5. Missense mutations in *MAM1* from mutant lines TU1 and TU5. The ORF of *MAM1* is presented as a bar. Vertical lines within this bar show exon-exon borders. Nucleotide substitutions causing missense mutations are shown above the bar. Numbering refers to the nucleotide sequence.

to individual members of a gene family, in the case of *GSL-ELONG*, screening of T-DNA insertion lines using populations available from the stock centers did not identify mutations in either *MAM1* or *MAM-L*. Therefore, we chose to exploit naturally occurring variation between Arabidopsis ecotypes to map *GSL-ELONG* at a fine scale.

In a cross between the Col-0 wild type and the recombinant inbred line CL5, a set of 4,600 F_2 plants (9,200 gametes) were scorable for recombination in the *GSL-ELONG* region. Because 1 cM equals approximately 200 kb in Arabidopsis, we expected to detect approximately one crossover per 2.3 kb in the 209-kb assayed region. The observed number of 95 recombinants (one crossover per 2.2 kb or 0.45 recombinants kb^{-1}) is almost exactly the number expected from the average relationship between physical distance and recombination frequency, indicating that fine-scale mapping can be a powerful tool to separate functional effects of tightly linked members of gene families, especially in the era of high-throughput genetics and genomics. However, crossover density varied significantly across the assayed interval, indicating recombination suppression near *GSL-ELONG* (Table I). This might be caused by differences in the organization of this region in the respective ecotypes and will be the subject of subsequent studies.

Due to this recombination suppression, approximately 5,000 F_2 plants were necessary to identify one recombinant separating the two adjacent genes of interest. Nevertheless, careful choice of F_1 plants generated a whole set of nearly isogenic lines harboring recombinations in the vicinity of *GSL-ELONG*. These lines can be used for fine quantitative trait locus mapping of many related traits in laboratory or field conditions, including glucosinolate quantity and insect resistance. Fine-scale mapping alone reduced the interval for candidate genes to less than 35 kb. In combination with heterologous expression in *E. coli* and the analysis of appropriate mutants, the gene responsible for C_3/C_4 chain length variation was unequivocally identified.

MATERIALS AND METHODS

Fine-Scale Mapping of *GSL-ELONG*

Arabidopsis ecotype Col-0 was crossed with the recombinant inbred line CL5 (Lister and Dean, 1993). CL5 is Col-0

WT for about 70% of the genome but harbors the L*er* allele at the *GSL-ELONG* locus. F_1 plants were verified for heterozygosity. F_2 plants were raised in 53 flats each containing 94 plants, in addition to Col-0 and L*er* WT plants, grown at a density of 337 plants/m^2 under 11.5-h/12.5-h light/dark cycles on a 1:3 (v/v) vermiculite:standard soil (Einheitserdenwerk, Fröndenberg, Germany) mix.

Total leaf DNA was isolated following a protocol modified from Edwards et al. (1991). Recombinants in the 209-kb region surrounding *GSL-ELONG* were identified with the primer pairs recMS1f/recMS1r and recMS9f/recMS9r using 3 μL from the DNA extract, 0.75 units of *Taq* polymerase (Qiagen, Hilden, Germany), 2 pmol of each primer of the first and 1 pmol of each primer of the second pair, and 5 nmol dNTPs in 23 μL of 1× Qiagen PCR buffer supplemented with MgCl$_2$. Cycling conditions were 94°C for 2 min followed by 38 cycles of 94°C for 15 s, 53°C for 15 s, and 72°C for 30 s, followed by 72°C for 5 min. The PCR fragments were fractionated on 6% (w/v) Metaphor agarose (Biozym, Hess. Oldendorf, Germany) gels or on an ABI 3700 DNA sequencer (PE Applied Biosystems, Sunnyvale, CA). In the latter case, recMS1f was 5′ labeled with 7′,8′-benzo-5′-fluoro-2′,4,7-trichloro-5-carboxyfluorescein, and recMS9f with 6-hexachlorofluorescein. Primers were obtained from MWG (Ebersberg, Germany), Metabion (Martinsried, Germany), or PE Applied Biosystems. Additional primer pairs used for fine-scale mapping were recMS2f/recMS2r, recMS5f/recMS5r, rec6f/rec6r, and recMS7f/recMS7r using reaction conditions similar to above. Finally, plants recom-
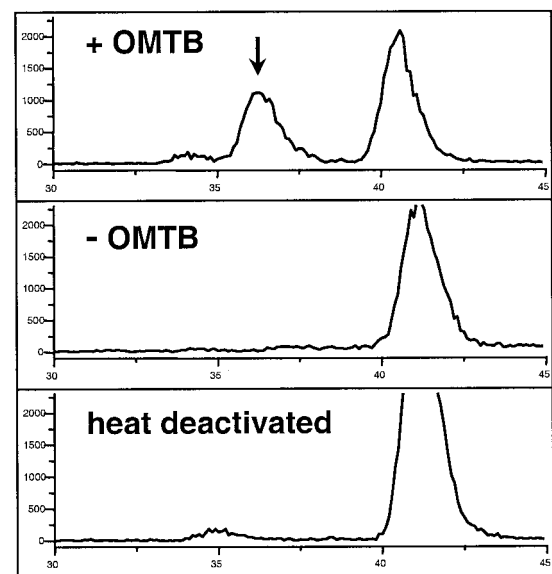

Figure 6. Cell-free enzyme assay of *E. coli* expressing the *MAM1* cDNA from Col-0. Cells were grown, extracted, and assayed with acetyl-CoA as described in "Materials and Methods." Pictured are radioactivity detector traces of the HPLC separations of assay products from 30 to 45 min. The upper trace represents the complete assay, including [1-^{14}C]acetyl-CoA and OMTB, and shows the production of MTEM (36.5 min), indicated by an arrow, and acetic acid (41 min), resulting from the hydrolysis of acetyl-CoA. The middle trace represents an assay without the cosubstrate OMTB, and the lower trace represents an assay with heat-denatured enzyme.

binant between rec6 and recMS7 were also analyzed with primer pairs EN-MSfor/EN-MSrev, Southex/16Cm2, and EDIT1-2a/11t1. Primers sequences were chosen from the Arabidopsis Col-0 *GSL-ELONG* region. Primer pairs recMS1f/recMS1r, recMS2f/recMS2r, recMS5f/recMS5r, recMS7f/recMS7r, recMS9f/recMS9r, and EN-MSfor/EN-MSr amplify polymorphic microsatellites. PCR products amplified from Col-0 and L*er* with rec6f/rec6r can be distinguished by a 72-bp insertion/deletion polymorphism. Col-0 and L*er* EDIT1 2a/11t1 and Southex/16Cm1 PCR products differ by several SNPs and 1-bp insertion/deletion polymorphisms that can be distinguished by sequencing. All primer sequences and marker sizes are listed in Table IV.

Extraction and Identification of Glucosinolates

Glucosinolates from Col-0 and L*er* wild-type, from the *gsm1* mutant lines TU1 and TU5 (Nottinhgam Arabidopsis Stock Centre [Nottingham, UK]/Arabidopsis Biological Resource Center, Ohio State University, Columbus; stock nos. CS2226 and CS2227, respectively) and L*er* × TU1 F_1 plants were extracted using boiling water as previously described (Graser et al., 2000). Plant material consisted of 0.05 g of lyophilized juvenile leaves of 5-week-old plants (approximately 10 plants). Samples were separated by HPLC (HP1100 Series, Agilent, Palo Alto, CA) fitted with a C-18 reverse-phase column using a water (Solvent A)-

acetonitrile (Solvent B) gradient at a flow rate of 1 mL min^{-1} and at ambient room temperature. The 42-min run consisted of 1.5% (v/v) B (1 min), 1.5% to 5.0% (v/v) B (5 min), 5.0% to 7.0% (v/v) B (2 min), 7.0% to 21.0% (v/v) B (10 min), 21.0% to 29.0% (v/v) B (5 min), 29.0% to 43.0% (v/v) B (7 min), 43.0% to 93.0% (v/v) B (0.5 min), a 4-min hold at 93.0% (v/v) B, 93.0% to 1.5% (v/v) B (0.5 min), and a 7-min hold at 1.5% (v/v) B. Eluent was monitored by diode array detection between 190 and 360 nm (2-nm interval). Glucosinolates were identified by retention time and UV spectra as compared with those of purified standards and quantified by $A_{229\ nm}$ relative to an internal standard (2-propenyl glucosinolate) included in the extraction. Response factors determined from pure desulfoglucosinolates for all compounds except 2-methylsulfinylethyl and 7-methylsulfinylheptyl glucosinolates (response factors assumed to be 1) were used to calculate molar concentrations of individual glucosinolates. Glucosinolates were extracted from the recombinant plants in a similar fashion except for modifications to facilitate high-throughput analyses. Lyophilized leaf samples (10 mg) were extracted in methanol and then treated essentially as described (Graser et al., 2000). The HPLC separation was carried out at 1 mL min^{-1} and the solvent program was modified as follows to accommodate high throughput analyses: 1.5% to 5.0% (v/v) B (6 min), 5.0% to 7.0% (v/v) B (2 min), 7.0% to 25.0% (v/v) B (7 min), 25.0% to 92.0% (v/v) B (2 min), 92.0% (v/v)

Table IV. *Primer sequences used in this study*
Size is indicated for PCR products used as genetic markers.

Primer Name	Sequence (5′ → 3′)	Size (Col-0)	Size (L*er*)
		bp	
recMS1f	GTGTGTCTATTAATATATCAAGAC	125	~120
recMS1r	GTTGTTTTATCTATGTTTATCAAG		
recMS2f	CCATTGGAGATGGTCTTACAC	107	~90
recMS2r	CTTTGTCACCAAGTCTTGTATAG		
recMS5f	GAATCAGATAATTAAGTTAGATAG	106	No product
recMS5r	GGTTCTTCATAAAAACAAAGCAC		
rec6f	GTGTAGTTTCATTTGTGCTATC	75	147
rec6r	CTTTAAAACTCTAAGCCTAGAC		
recMS7f	CATAAGATGGAAGCGTTAGAC	132	~150
recMS7r	GATGGTAAACTACTTTGTGAAC		
recMS9f	GGTTCCAAGTTACAAACTTTAAC	105	~90
recMS9r	CGACCTAACGGCAAGTGAAAG		
EN-MSfor	CATGAGAGCGGCATTCACCAG	100	88
EN-MSrev	GGACAATTATACACATACAACGC		
16Cm2	GGGCTTATGTGCTTGAAC	430	430
Southex	GAAATGTCGAGGGGCATATG	SNPs, 1-bp indels	SNPs, 1-bp indels
EDIT1-2a	GTACCACAGTAATATCAATTTCC	207	208
11t1	GTTCATGAGATATGAGTAAGTGG	SNPs, 1-bp indel	SNPs, 1-bp indel
C/L-ESfEE	ATATGAATTCAACTATGTGCGTGTATTCGAC	–	–
CESrEE	ATATCTCGAGCACATTCGATGAAACCTGAGG	–	–
L-ENfEE	ATATGGATCCTATGTGCGTGTATTAGACAC	–	–
L-ENrEE	ATATCTCGAGTACAACAGCGGAAATCTGAGG	–	–
IPMS0	CACCGTCACGTTGAAACCTTC	–	–
E116r	TTTTTAATTCAGGCAGCGACTCT	–	–
1MAM1a	ACTCCATAGTGATGGCTTCATCGCTTCTG	–	–
2MAM1b	AGAGATACAACGTGTTTACACATTC	–	–
1MAMLa	TATAGTAATGGCTTCGTTACTTCTC	–	–
2MAMLb	TCTTCCCAAACTTATACAACAGCG	–	–

B (6-min hold), 92.0% to 1.5% (v/v) B (2 min), and 1.5% (v/v) B (5 min).

Amplification of cDNAs

Total plant RNA was isolated with Trizol (Gibco-Invitrogen, Karlsruhe, Germany) according to the manufacturer's recommendations. First strand cDNA was synthesized following a protocol modified from Frohman et al. (1988). A cDNA corresponding to *F15H18.3* was amplified using 1 μL of first strand product derived from Col-0 using primers IPMS0 and E116r (Table IV). The cDNAs corresponding to the entire ORFs of *MAM1* and *MAM-L* from both TU1 and TU5 were synthesized in a 33-μL reaction mix consisting of 1$\times$ TaKaRa (TaKaRa, Japan) reaction buffer, 8.5 nmol of dNTPs, and 10 pmol of the primer pairs 1MAM1-a/2MAM1-b and 1MAMLa/2MAMLb, respectively. Reaction products were gel purified (QiaQuick, Qiagen). In each case, reactions were performed three times, and PCR products were sequenced on an ABI 3700 DNA sequencer with Big Dye Terminators (PE Applied Biosystems). Assembly and comparison of DNA sequence data was done using LASERGENE software (DNASTAR, Inc., Madison, WI) or GCG (version 10).

Expression Constructs

MAM1 cDNAs from both Col-0 and L*er* were amplified with the primer pair C/L-ESfEE/CESrEE (Table IV). These primers were chosen to truncate the first 246 nucleotides that appear to represent an N-terminal signal sequence and thus could hamper expression in a prokaryotic system. The PCR products were gel purified (Qiagen) and cloned into pCR2.1-TOPO (Invitrogen, Breda, The Netherlands). Insert sequences were verified by sequencing. Suitable *MAM1* inserts were excised with *Eco*RI and *Xho*I and recloned directionally into a pET-28a expression vector (Novagen, Madison, WI). An expression construct encoding the mutant allele from TU1 was obtained by site-directed mutagenesis of the functional *MAM1* expression construct from Col-0 using a QuikChange Site-Directed Mutagenesis Kit (Stratagene, La Jolla, CA). Expression constructs of *MAM-L* were prepared by similar methods with cDNAs amplified by the primer pair L-ENfEE/L-ENrEE.

cDNA Expression in *Escherichia coli*

The *MAM1* and *MAM-L* constructs were expressed in *E. coli* strain BL21(DE) (F$^-$ ^{ompT} $r_B^-$$m_B^-$; (Studier et al., 1990) grown in M9 medium with acid-hydrolyzed casein to an optical density at 600 nm of 0.6 and then induced with 1 mM isopropylthio-β-galactoside for 2 h. Cells were harvested by centrifugation at 6,500g. After resuspension in 50 mM Tris, pH 8.0, with 1 mM dithiothreitol, cells were sonicated with a Sonoplus HD2070 sonicator (Bandelin, Berlin) twice with a microprobe at 55% full power for a 5-min −20% cycle. Cell debris was precipitated by centrifugation at 8,500g and the supernatant used for the enzyme assays.

Enzyme Assay

The assay mixture contained 100 mM AMPSO, pH 9.0, 4 mM MnCl$_2$, 1 mM [1-^{14}C]acetyl-CoA (14.8 GBq mol^{-1}), 20 mM ATP, 3 mM OMTB, and 150 μL of enzyme preparation in a final volume of 250 μL. After an incubation period of 16 h at 32°C, the reaction was stopped by the addition of 750 μL of ethanol and denatured protein precipitated by centrifugation. The supernatant was concentrated to a volume of about 50 μL for HPLC analysis. An ion exclusion column (Nucleogel ion-300 OA, Macherey and Nagel, Düren, Germany) was run isocratically with 0.005 N H$_2$SO$_4$ at a flow rate of 0.25 mL min^{-1}, 60°C, for 45 min. Detection employed a flow-through radioactivity monitor (Radiomatic 500TR, Packard, Dreieich, Germany) with a 0.5-mL flow cell and Ultima-Flo AP scintillation fluid (Packard) in a ratio of 4:1 (v/v) to column eluent. The counting efficiency for ^{14}C was 55% to 60%. Under these conditions, the reaction product, MTEM, eluted at approximately 36.5 min, well separated from the substrates, acetyl-CoA (16.5 min) and OMTB (28 min), and from free acetate (41 min).

Product Identification

The assay product was identified with a liquid chromatography-MS system using a Quattro II (Micromass, Altrincham, UK) tandem quadrupole mass spectrometer equipped with an electrospray interface (capillary, 2.5 kV; sample cone, 12 V; and desolvation temperature, 375°C). The HPLC conditions were as described above except that the solvent was 0.03% (v/v; aqueous) CF$_3$COOH and the flow rate was 0.2 mL min^{-1}. The MS-MS spectra were recorded by fragmentation of the [M + H]$^+$ parent ion at m/z 209. Argon was used as the collision gas at 1.4 $\times$ 10^{-3} mbar, and a collision energy of 7 eV was employed to achieve fragmentation. The scanned mass range was m/z 50 to m/z 215 and the scan time 1 s. The biosynthetic product gave a mass spectrum identical to that of synthetic MTEM prepared by methods previously described (Chapple et al., 1988).

Cluster Analysis of IPMS-Like Sequences in Arabidopsis

Alignments of IPMS-like sequences were carried out with DNASTAR (Lasergene), and corrected manually. A neighbor-joining tree (Saitou and Nei, 1987) was constructed with TREECON (van de Peer and de Wachter, 1994) taking into account residues 27 through 392 of the derived IPMS protein sequence from *Methanococcus* sp. and the corresponding amino acids from other IPMS-like proteins, and using an algorithm for distance estimation developed by Tajima and Nei (1984). Reliability of the branching order was estimated by bootstrapping (100 replicates; Felsenstein, 1985). GenBank accessions numbers are: AAB99199 (*Methanococcus jannaschii*), BAA10079 (*Synechocystis* sp.), AF004165 (tomato [*Lycopersicon pennellii*] IPMSa), AF004166 (tomato IPMSb), AC016662 (F2P9.9), AC013354 (F15H18.3), AB006708 (*MAM-L*), and AB026660 (MAM1).

ACKNOWLEDGMENTS

LITERATURE CITED

Blau PA, Feeny P, Contardo L (1978) Allylglucosinolate and herbivorous caterpillars: a contrast in toxicity and tolerance. Science **200:** 1296–1298

Bodnaryk RP (1991) Developmental profile of sinalbin (*p*-hydroxybenzyl glucosinolate) in mustard seedlings, *Sinapis alba* L., and its relationship to insect resistance. J Chem Ecol **17:** 1543–1556

Bones AM, Rossiter JT (1996) The myrosinase-glucosinolate system, its organization and biochemistry. Physiol Plant **97:** 194–208

Bradshaw JE, Heaney RK, Smith WHM, Gowers S, Gemmell DJ, Fenwick GR (1984) The glucosinolate content of some fodder brassicas. J Sci Food Agric **35:** 977–981

Brown PD, Morra MJ (1995) Glucosinolate-containing plant tissues as bioherbicides. J Agric Food Chem **43:** 3070–3074

Campos H, Magrath R, McCallum D, Kroymann J, Schnabelrauch D, Mitchell-Olds T, Mithen R (2000) α-Keto acid elongation and glucosinolate biosynthesis in *Arabidopsis thaliana*. Theor Appl Genet **101:** 429–437

Chapple CC, Decicco C, Ellis BE (1988) Biosynthesis of 2-(2'-methylthio) ethylmalate in *Brassica carinata*. Phytochemistry **27:** 3461–3463

Chapple CC, Glover JR, Ellis BE (1990) Purification and characterization of methionine-glyoxylate aminotransferase from *Brassica carinata* and *Brassica napus*. Plant Physiol **94:** 1887–1896

Chisholm MD, Wetter LR (1964) Biosynthesis of mustard oil glucosides: IV. The administration of methionine-C^{14} and related compounds to horseradish. Can J Biochem **42:** 1033–1040

Donkin SG, Eiteman MA, Williams PL (1995) Toxicity of glucosinolates and their enzymatic decomposition products to *Caenorhabditis elegans*. J Nematol **27:** 258–262

Doughty KJ, Porter AJR, Morton AM, Kiddle G, Bock CH, Wallsgrove R (1991) Variation in the glucosinolate content of oilseed rape (*Brassica napus* L.) leaves: response to infection by *Alternaria brassicae* (Berk.) Sacc. Ann Appl Biol **118:** 469–477

Du YJ, van Loon JJA, Renwick JAA (1995) Contact chemoreception of oviposition-stimulating glucosinolates and an oviposition-deterrent cardenolide in two subspecies of *Pieris napi*. Physiol Entomol **20:** 164–174

Edwards K, Johnstone C, Thompson C (1991) A simple and rapid method for the preparation of plant genomic DNA for PCR analysis. Nucleic Acids Res **19:** 1349

Emanuelsson O, Nielsen H, von Heijne G (1999) ChloroP, a neural network-based method for predicting chloroplast transit peptides and their cleavage sites. Prot Sci **8:** 978–984

Fahey JW, Zhang Y, Talalay P (1997) Broccoli sprouts: an exceptionally rich source of inducers of enzymes that protect against chemical carcinogens. Proc Natl Acad Sci USA **94:** 10367–10372

Felsenstein J (1985) Confidence limits on phylogenies: an approach using the bootstrap. Evolution **39:** 783–791

Frohman MA, Dush MK, Martin GR (1988) Rapid production of full-length cDNAs from rare transcripts: amplification using a single gene-specific oligonucleotide primer. Proc Natl Acad Sci USA **85:** 8998–9002

Giamoustaris A, Mithen R (1995) The effect of modifying the glucosinolate content of leaves of oilseed rape (*Brassica napus* ssp. *oleifera*) on its interaction with specialist and generalist pests. Ann Appl Biol **126:** 347–363

Graser G, Schneider B, Oldham NJ, Gershenzon J (2000) The methionine chain elongation pathway in the biosynthesis of glucosinolates in *Eruca sativa* (Brassicaceae). Arch Biochem Biophys **378:** 411–419

Hagelstein P, Schultz G (1993) Leucine synthesis in spinach chloroplasts: partial characterization of 2-isopropylmalate synthase. Biol Chem Hoppe Seyler **374:** 1105–1108

Hagelstein P, Sieve B, Klein M, Jans H, Schultz G (1997) Leucine synthesis in chloroplasts: leucine/isoleucine aminotransferase and valine aminotransferase are different enzymes in spinach chloroplasts. J Plant Physiol **150:** 23–30

Halkier BA, Du L (1997) The biosynthesis of glucosinolates. Trends Plant Sci **11:** 425–431

Halkier BA (1999) Glucosinolates. *In* R Ikan, ed, Naturally Occurring Glycosides: Chemistry, Distribution and Biological Properties. John Wiley and Sons, Chichester, UK, pp 193–223

Haughn GW, Davin L, Giblin M, Underhill EW (1991) Biochemical genetics of plant secondary metabolites in *Arabidopsis thaliana*: the glucosinolates. Plant Physiol **97:** 217–226

Hogge LR, Reed DW, Underhill EW, Haughn GW (1988) HPLC separation of glucosinolates from leaves and seeds of *Arabidopsis thaliana* and their identification using thermospray liquid chromatography-mass spectrometry. J Chromatogr Sci **26:** 551–556

Kliebenstein DJ, Kroymann J, Brown P, Figuth A, Pedersen D, Gershenzon J, Mitchell-Olds T (2001) Genetic control of natural variation in *Arabidopsis thaliana* glucosinolate accumulation. Plant Physiol **126:** 811–825

Justus KA, Mitchell BK (1996) Oviposition site selection by the diamondback moth, *Plutella xylostella* (L.) (Lepidoptera: Plutellidae). J Insect Behav **9:** 887–898

Lister C, Dean C (1993) Recombinant inbred lines for mapping RFLP and phenotypic markers. Plant J **4:** 745–750

Magrath R, Bano F, Morgner M, Parkin I, Sharpe A, Lister C, Dean C, Turner J, Lydiate D, Mithen R (1994) Genetics of aliphatic glucosinolates: I. Side chain elongation in

Brassica napus and *Arabidopsis thaliana*. Heredity **72:** 290–299

Matsuo M, Yamazaki M (1964) Biosynthesis of sinigrin. Chem Pharmacol Bull **12:** 1388–1389

Mithen R, Clarke J, Lister C, Dean C (1995) Genetics of aliphatic glucosinolates: III. Side chain structure of aliphatic glucosinolates in *Arabidopsis thaliana*. Heredity **74:** 210–215

Nastruzzi C, Cortesi R, Esposito E, Menegatti E, Onofrio L, Iori R, Palmieri S (1996) *In vitro* cytotoxic activity of some glucosinolate-derived products generated by myrosinase hydrolysis. J Agric Food Chem **44:** 1014–1021

Rask L, Andreasson E, Ekbom B, Eriksson S, Pontoppidan B, Meijer J (2000) Myrosinase: gene family evolution and herbivore defense in Brassicaceae. Plant Mol Biol **42:** 93–113

Reed DW, Pivnick KA, Underhill EW (1989) Identification of chemical oviposition stimulants for the diamondback moth, *Plutella xylostella*, present in three species of Brassicaceae. Entomol Exp Appl **53:** 277–286

Saitou N, Nei M (1987) The neighbor-joining method: a new method for reconstructing phylogenetic trees. Mol Biol Evol **4:** 406–425

Städler E, Renwick JAA, Radke CD, Sachdev-Gupta K (1995) Tarsal contact chemoreceptor response to glucosinolates and cardenolides mediating oviposition in *Pieris rapae*. Physiol Entomol **20:** 175–187

Studier FW, Rosenberg AH, Dunn JJ, Dubendorf JW (1990) Use of T7 RNA polymerase to direct expression of cloned genes. Methods Enzymol **185:** 60–89

Tajima F, Nei M (1984) Estimation of evolutionary distance between nucleotide sequences. Mol Biol Evol **1:** 269–285

van de Peer Y, de Wachter R (1994) TREECON for Windows: a software package for the construction and drawing of evolutionary trees for the Microsoft Windows environment. Comput Appl Biosci **10:** 569–570

von Heijne G, Steppuhn J, Herrmann RG (1989) Domain structure of mitochondrial and chloroplast targeting peptides. Eur J Biochem **189:** 535–545

Zhang GY, Talalay P, Cho C, Posner GH (1992) A major inducer of anticarcinogenic protective enzymes from broccoli: isolation and elucidation of structure. Proc Natl Acad Sci USA **89:** 2399–2403